JOURNAL OF CATALYSIS 1, 136–150 (1962)

Semiconductivity and Catalytic Activity. The Dehydrogenation of Isopropyl Alcohol on $ZnO–Cr_2O_3$ Catalysts

JUAN F. GARCÍA DE LA BANDA

From the Instituto de Química Física "Rocasolano," Madrid, Spain

Received October 26, 1961

Kinetics of isopropyl alcohol dehydrogenation on Cr_2O_3 prepared by decomposition of the corresponding hydroxide in air at 400°C has been studied. Experimental results point to a change in the semiconductor type of the Cr_2O_3 catalyst during the reaction.

In order to confirm this hypothesis, the H_2 and O_2 adsorption on both types of Cr_2O_3, as well as the modification of the electrical resistance, at constant temperature, versus hydrogen pressure and versus feed during the reaction have been studied. Results are in agreement with the existence of two forms of Cr_2O_3 which, in principle, behave as p (oxidized form) and n (reduced form) semiconductors.

The study of isopropyl alcohol dehydrogenation kinetics on $ZnCr_2O_4$ leads us to the conclusion that this possible $p \rightarrow n$ transition is not a quality which is exclusive for Cr_2O_3.

These points are discussed and their importance and possible implications on future work duly considered.

INTRODUCTION

The study of the relationships between the electronic structure of solid catalysts and their catalytic activity is extremely interesting. Very fine work has been accomplished by different schools and some very good reviews have been published during the last few years on this topic (*1*).

We are not going to discuss this subject in a general way, but will restrict ourselves to a particular aspect. As we will see later on, this aspect is not altogether new but it has been studied in some detail, which has allowed us to confirm some well established ideas and to postulate a few new ones.

Past work, undertaken by Garner and co-workers (*2*), in which isopropyl alcohol dehydrogenation on different catalysts of the $ZnO–Cr_2O_3$ series is employed as reference reaction, shows that high dehydrogenation activity is associated with the n-type, quasi-metallic, ZnO-rich catalysts. A rough proportionality between the logarithm of the electrical conductivity in a hydrogen atmosphere and the specific activity of those catalysts was found.

These results were confirmed by the study of the electrical conductivity in the $ZnO–Cr_2O_3—K_2CrO_4$ series (*3*) during isopropyl alcohol dehydrogenation. General evidence obtained in this reaction is consistent with the hypothesis of an electron acceptor rate-determining step (*4*). During our work it was found that at 480°C the direction of change in electrical conductivity of a potassium-doped $ZnCr_2O_4$ pellet with time, at constant temperature and reactant feed, was the reverse of that for 410°C. This fact was tentatively explained assuming a $p \rightarrow n$ change in the semiconductor character of $ZnCr_2O_4$ during the reaction. A very interesting finding is that, catalyst activity does not change during these experiments. In other words, for constant temperature and reactant feed, conductivity changes with time but activity remains constant.

The mechanism which has been suggested for this reaction was discussed, together with that reported by Hauffe (*5*), on the basis of semiconductivity–activity considerations (*6*). Experimental evidence pointed to the desorption of acetone as the rate-determining step.

With the aim of obtaining information on the reaction mechanism, the kinetics of the isopropyl alcohol dehydrogenation on ZnO was studied using a differential reactor. Results were not in agreement with the previous hypothesis (*7*).

Considering that ZnO is a typical *n*-type semiconductor it was hoped that kinetic studies on Cr_2O_3, which roughly behaves as a *p*-type semiconductor, would cast some light on the mechanism of this reaction. As we will see further on, the results found promoted researches relating to the reaction kinetics on $ZnCr_2O_4$, semiconductivity changes in different atmospheres and adsorption.

EXPERIMENTAL

Kinetics on Cr_2O_3

The catalyst used in this work was prepared from $Cr(NO_3)_3$ BDH Laboratory Reagent.

A $Cr(NO_3)_3$ solution in distilled water was partially precipitated with a small amount of Merck analytical grade NH_4OH, in order to eliminate possible traces of iron. The filtrate was heated to about 80°C and the chromium precipitated, with Merck analytical grade NH_4OH, in the form of $Cr(OH)_3$. The precipitate was washed with boiling distilled water until all NO_3^- ions were eliminated, and then dried at 100–110°C during several hours, following which Cr_2O_3 was obtained by decomposition at 400°C during 4 hr in air.

The Cr_2O_3 obtained was sintered at 600°C during 4 hr in air and then sieved in the 0.074 to 0.053 DIN range. For a part of the work 0.60-cm diameter cylindrical pellets weighing approximately 0.5 g were obtained from sieved Cr_2O_3 powder, and sintered in the same way.

Details of the apparatus and experimental technique are given elsewhere (*7–10*). Nevertheless in order to give a more lucid illustration of our work we shall expand on the fundamental details up to the point of being able to omit references on original developments.

During our work on ZnO (*7*), we excluded external diffusion using a high enough reactant flow but, due to the fact that we used cylindrical pellets, internal diffusion was significant and a very low value of the apparent activation energy was found.

In order to overcome this difficulty, in this work (*8*) we employed almost the same differential reactor although, in every possible case, we used powdered catalyst in an amount adequate to ensure that the reaction rate varied linearly in terms of the catalyst mass.

Description of the Apparatus

Figure 1 illustrates the set up for the apparatus, the main parts of which are the following:

a. A capillary system to achieve constant liquid flow.
b. A boiler and a homogeneous mixing and preheating device.
c. Furnace, preheater, and reaction chamber.
d. A device for the separation and measurement of the gaseous products.
e. A device for the obtention, purification, and measurement of hydrogen.

These individual parts are now briefly described.

Capillary system. This consists essentially of three capillaries, provided with a system of stopcocks, which can be adjusted to obtain seven different flow rates.

Both the isopropyl alcohol, or the isopropyl alcohol–acetone mixture under consideration are kept at constant level and the capillaries are covered with melting ice; consequently a constant flow of liquid is obtained. Using tap water ice the liquid flow is constant to within ±1%. Using distilled water ice constancy increases to ±0.1%.

Boiler and device for homogeneous mixing and preheating. The boiler is cylindrical in shape and located vertically with a coaxial capillary (internal diameter, 1 mm) which communicates with the capillary system. The boiler is heated with an electrical resistance coil, the loops of which are more closely wound near the top of the boiler.

For a constant liquid flow, it boils inside the capillary at a given height, which depends on the flow rate and temperature distribution in the boiler (which, in its turn is changed by controlling the current in the electrical heater). With this system a perfectly controlled even boiling is achieved giving rise to a constant vapor flow.

The isopropyl alcohol–acetone vapors, can be mixed with hydrogen, and preheated in the proximity of the reaction temperature.

All heating operations are effected with electrical resistances and the whole system is thermally insulated. Great care has been taken to ensure this, since in the boiler and, within certain limits in every part of the system, constancy of the temperature must be critical in order to keep a constant apparent volume in the apparatus, especially when hydrogen mixtures are used (*10*). We must point out that one of the most important sources of error is sudden temperature change, while long period changes are irrelevant.

Furnace, preheater, and reaction chamber. The furnace has an iron tube core and three independent windings, in order to ensure a uniform temperature in as large a region as possible.

Before entering the reaction chamber the gaseous mixture passes through a glass coil located inside the furnace. This coil operates as a preheater.

The reaction chamber is a 4-cm ID Pyrex tube, one end of which is connected to the preheater and the other closed by a standard joint. In this standard joint we inserted two tubes, one for a thermocouple and another for the evacuation of the products. A tray of 0.053 DIN copper alloy screen, which supports the catalyst, is located in the internal end of this last tube. The reactant vapors flow perpendicular to this tray.

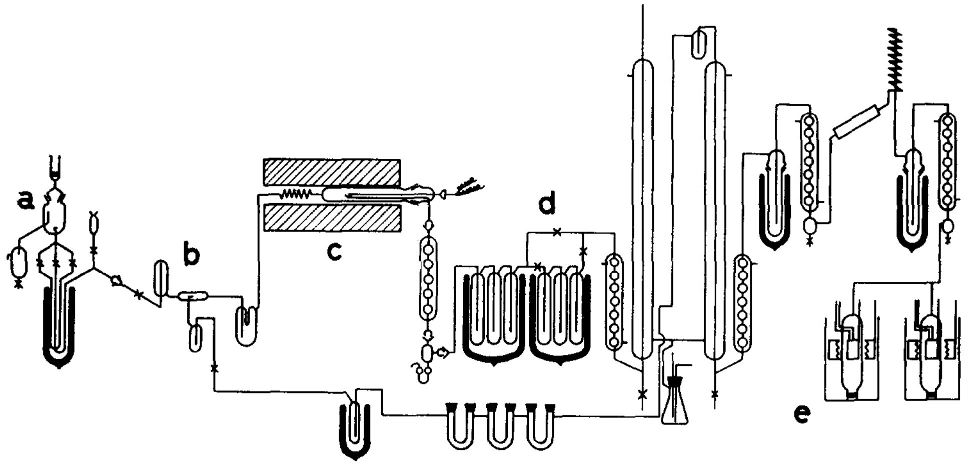

FIG. 1. Schematic diagram of the apparatus for measuring reaction rates: a—capillary system; b—boiler mixer and preheater; c—furnace and reaction chamber; d—device for the separation and measurement of gaseous products; e—device for the obtention, purification and measurement of hydrogen.

When pellets are used, one of their bases rests on the bottom of the region where the screen would be situated in the internal end of the exit tube.

The temperature of the furnace was kept constant within less than ±0.5°C.

Device for the separation and measurement of the gaseous products. The reactants which have not reacted and the products abandoning the furnace proceed first to a cool water condenser and then to a series of three salt–ice freezing mixture traps. The gaseous flow is sent to a series of three liquid-air-cooled traps.

The volume of gas obtained per unit time can be measured using a water-jacket thermostabilized soap bubble burette. Before being introduced into the measuring burette the gas (hydrogen in this case) flows through a heat exchanger, where it is heated to the temperature of the measuring burette water jacket.

Device for the obtention, purification, and measurement of hydrogen. Hydrogen was obtained electrolytically using a two cell battery arrangement. Voltage was supplied by a high capacity lead storage battery through a potentiometric system.

The hydrogen obtained is first passed through a cold water condenser; then through a liquid-air-cooled trap and, finally, after being heated at room temperature, to a "Deoxo" (from Baker Platinum Ltd.).

The amount of hydrogen produced per minute is measured employing a soap bubble burette. Before entering the apparatus the hydrogen flows over silica gel through a liquid air trap.

Measuring Procedure and Results

Prior to the initiation of the measurements we must check the performance of every single part of the apparatus.

Besides reactant flow constancy, normal routine check between runs include the following experiment:

The different parts of the apparatus are heated up to the running temperature, except for the furnace, which must be kept at a constant value in the 200–250°C range. All traps are cooled with the corresponding freezing mixtures to the correct levels (in order that the trap bulbs be fully covered).

In the absence of catalyst a constant flowing isopropyl alcohol–acetone mixture is sent through the apparatus and mixed with hydrogen.

In this condition, the hydrogen flows measured at the entrance and outlet of the apparatus must be equal to each other with an approximation of ±0.1%.

The measurements were started for different weights of Cr_2O_3 powder in order to verify whether the hydrogen production is proportional to the weight of the catalyst. Figure 2 illustrates the results obtained using pure isopropyl alcohol. These results seem to adjust themselves accurately enough to a straight line up to catalyst weights of ~0.01 g at all the temperatures studied. For higher catalyst weights activity is lowered due to the effect of internal diffusion limitations.

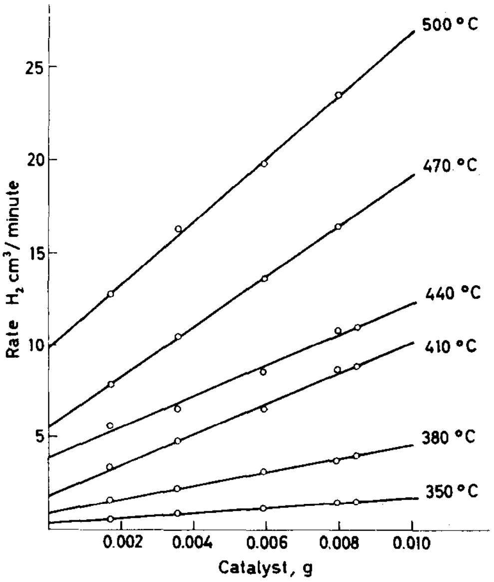

FIG. 2. Isopropyl alcohol dehydrogenation rate on Cr_2O_3 catalyst.

The same kind of plots were found for several isopropyl alcohol–acetone reaction mixtures in the pure isopropyl alcohol to 60 moles of isopropyl alcohol/100 moles of mixture range.

The values at the origin represent the activities of the screen and of the apparatus. These may be kept constant using the same screen for each mixture for all catalyst weights and temperatures. In order to maintain standard operating conditions the screen must be carefully cleaned after each run. The cleaning procedure resorted to in this study involves the use of a compressed air jet and surface reduction with methyl alcohol under vacuum.

From plots such as that of Fig. 2 it is easy to estimate the catalytic activity per gram of powdered catalyst. Complete tables of experimental values may be found in references (*8*) and (*10*). They are not given in this paper as we do not consider it necessary for our ends.

The next set of experiments, using isopropyl alcohol–hydrogen mixtures was initiated employing a technique identical to that for the case of the isopropyl alcohol–acetone mixtures.

It was soon realized that, due to the strong inhibitive effect of hydrogen, the weight of the catalyst had to be considerably increased in order to obtain measurable reaction rates. However, due to the internal diffusion, the linearity of the H_2 cm^3/minute versus Cr_2O_3 weight plot is soon lost when the weight of the catalyst is increased until suitable easily and accurately measurable reaction rate values are obtained. Therefore, for hydrogen-containing mixtures we decided to employ a modification of the pellets technique used in the study of isopropyl alcohol dehydrogenation on ZnO (*7*).

Using hydrogen-containing mixtures it is very easy to work in the flow region in which external diffusion is not important. In order that with pellets we may obtain results comparable to those obtained with powder the following procedure was used. For every temperature, the measurement of the reaction rate for a given isopropyl alcohol–acetone–hydrogen mixture, was preceded by a determination of the apparent reaction rate of the pellet in the said isopropyl alcohol–acetone mixture in the absence of hydrogen. The comparison of these apparent reaction rates with those obtained for powdered Cr_2O_3, allows us to estimate the latter, on the basis of apparent reaction rate measurements obtained for pellets and hydrogen-containing mixtures.

In theoretical support of this method we need only assume that, for a given composition of the isopropyl alcohol–acetone mixture, the effectiveness factor of the pellet is independent of the amount of hydrogen added. This seems to be a plausible assumption, at least in the instance of not very high hydrogen partial pressures.

As a complementary precaution, in order to maintain similar geometrical conditions, work was carried out with pellets of the same size and weight, and identically located inside the reaction chamber. Throughout the measurements, the total flow was also kept at a constant value from which previous experience shows that the influence of external diffusion has been eliminated.

Results obtained for isopropyl alcohol–hydrogen mixtures at these different temperatures are of the shape shown in Fig. 3. As the partial pressure of hydrogen increases, the curves exhibit a minimum followed by a maximum. The same kind of plot has been found for all the isopropyl alcohol–acetone initial mixtures when the amount of hydrogen added to the feed increases. Tables of experimental values are given in references (*8*) and (*10*).

The study of the rate equation was undertaken exclusively on the basis of the reaction rate and partial pressure values corresponding to the region immediately preceding the minimum. The detailed study of the possible rate equations (*9, 10*) in the low hydrogen partial pressure range shows that the most probable mechanism is the same as in the case of ZnO (*7*). Therefore the apparent mechanism involves two equal active centers (possibly oxygen ions). Isopropyl alcohol, acetone, and hydrogen are adsorbed and the surface reaction is the rate-determining step.

The rate equation corresponding to this apparent mechanism is:

$$V = \frac{k'CK_A}{(1 + K_A f_A + K_R f_R + K_S f_S)^2} \left(f_A - \frac{f_R f_S}{K}\right) \quad (1)$$

where:

f_i = fugacity of component i
K_i = adsorption equilibrium constant of component i
k' = forward reaction velocity constant
K = overall equilibrium constant
C = a proportionality constant

Throughout the whole paper we employ the following subscripts: A = isopropyl alcohol, R = acetone, and S = hydrogen.

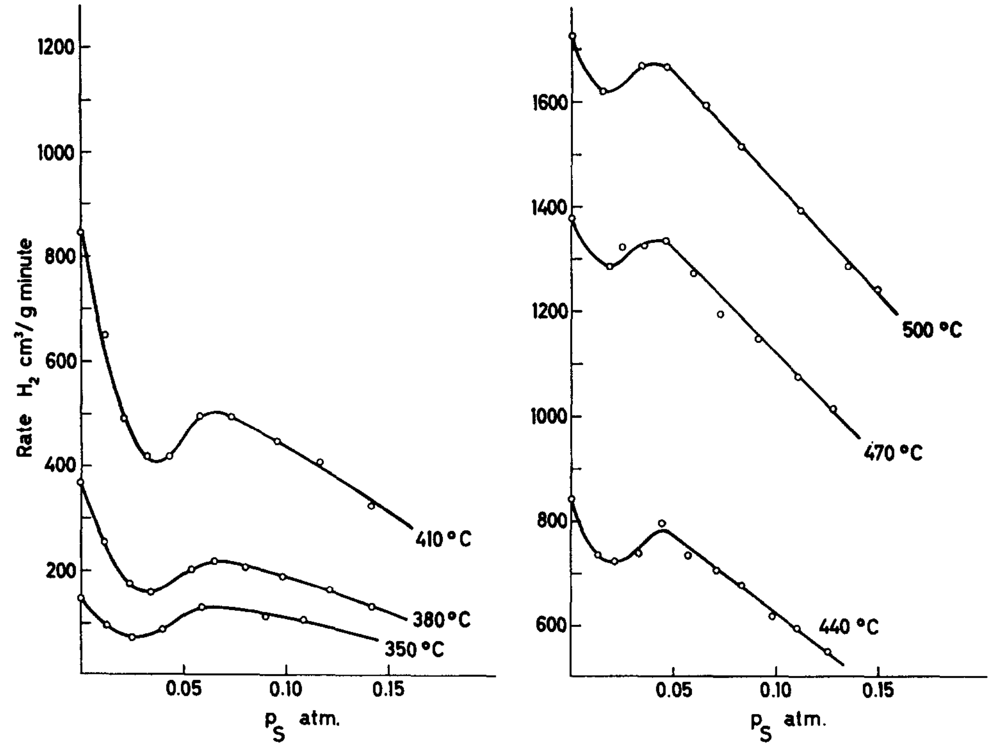

FIG. 3. Reaction rate on Cr_2O_3 catalyst versus hydrogen partial pressure. Isopropyl alcohol-hydrogen mixture feed.

Due to the fact that all the experiments have been carried out at almost constant pressure, and that we can only use the experimental points corresponding to the region preceding the minimum, it has not been possible to calculate $k'C$, K_A, K_R, and K_S separately. We have used a simplified form of Eq. (1) with three parameters which are simple functions of $k'C$, K_A, K_R, and K_S. Tables of values are given, for the different temperatures, in references (*9*) and (*10*).

Another interesting aspect is that in the case of all the initial mixtures studied the Arrhenius plot has the shape shown in the Fig. 4. In this particular case the experiments were carried out with pure isopropyl alcohol feed. The slope of the Arrhenius straight lines for all isopropyl alcohol-acetone mixtures is the same. In his very useful critical analysis of data obtained using differential reactors (*11*) Germain believes that this fact comes in support of the nonexistence of internal diffusion.

At this point we have something to say in connection with the temperature measurements during our work. We measure the temperature in the gaseous flow next to the catalyst; therefore there is a gradient of temperature and the surface of the

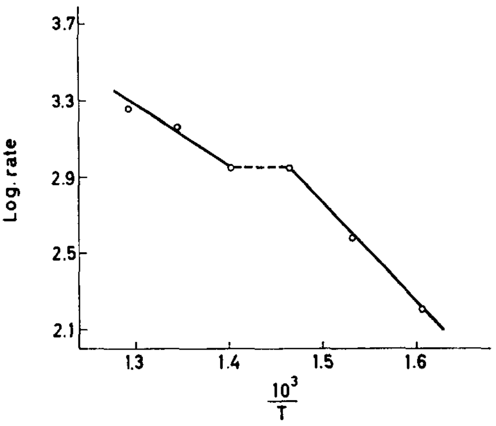

FIG. 4. Dehydrogenation on Cr_2O_3 catalyst. Arrhenius plot.

catalyst must be cooler on account of the endothermicity of the reaction. Nevertheless, taking Germain's data (*11*) into account it seems plausible that, at least for the powder, the difference should not be too high. In the case of pellets the actual rate of reaction is low, less than 1000 H_2 cm^3/hr, which, together with lack of external diffusion limitations, points to a moderate temperature gradient.

Kinetics on $ZnCr_2O_4$

The kinetics of isopropyl alcohol dehydrogenation on $ZnCr_2O_4$ has been studied by Kremenić (*12*). The chemicals employed are the same as those used in the kinetic study on ZnO and Cr_2O_3 catalysts. The experimental technique was the same as that already described.

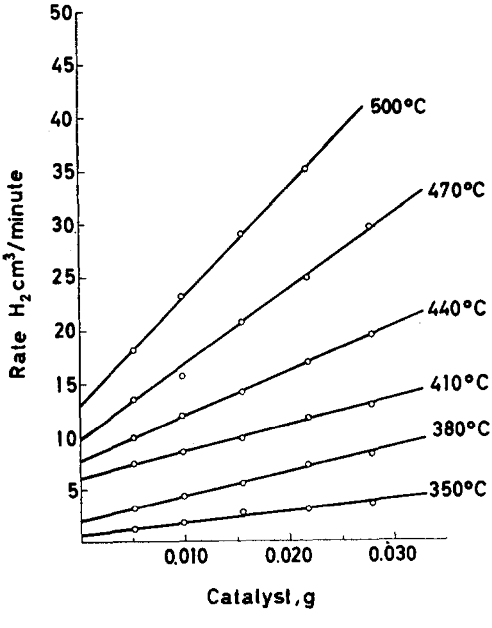

FIG. 5. Isopropyl alcohol dehydrogenation rate on $ZnCr_2O_4$ catalyst.

The $ZnCr_2O_4$ catalyst was prepared in the usual way by coprecipitation of the hydroxides, their subsequent decomposition to oxides, and sintering at 800°C during 4 hr in air. X-ray control shows that under these conditions a good crystalline spinel was formed.

Figure 5 shows the results obtained with pure isopropyl alcohol feed. The same kind of plots were found for isopropyl alcohol–acetone mixtures ranging from pure isopropyl alcohol to 60 moles of isopropyl alcohol/100 moles of mixture. Results seem to adjust themselves accurately enough to a straight line up to catalyst weights of 0.02 g and for every temperature.

Results for hydrogen-containing mixtures have the shape shown in Fig. 6, with isopropyl alcohol–hydrogen feed mixtures. The shape is the same as that obtained with Cr_2O_3 catalyst, but the minimum appears at a lower hydrogen partial pressure.

From the study of the rate equations at low hydrogen partial pressure (experimental points preceding the minimum) it seems that the mechanism on $ZnCr_2O_4$ is the same as for Cr_2O_3. Considering that the p_S values for which the minimum is recorded are much smaller than in the case of the Cr_2O_3 catalyst, the degree of certainty is lower, and we have not attempted to calculate the reaction rate coefficients.

The break in the Arrhenius plot, see Fig. 7, takes place in the 380–410°C range. The slope of the Arrhenius straight lines for all the isopropyl alcohol–acetone mixtures is the same.

Adsorption of H_2 and O_2 on Cr_2O_3

Azcue (*13*) studied the adsorption of H_2 and O_2 both on oxidized and reduced Cr_2O_3. The experimental setup involves an all-in-glass scale located in a glass case connected to gas handling and vacuum systems.

The end of the scale arms are provided with two condenser plates in series. The other two plates are fixed to the scale case. These plates are connected to a capacity analyzer through tungsten-Pyrex seals.

One arm of the scale sustains a pan and the other a glass covered permanent magnet. This magnet is located in the axis of an external coil.

When the scale is in equilibrium, the condensers have a certain capacity. If the scale is displaced from the equilibrium position this capacity changes and the electronic system sends through the coil the necessary current to return the scale to

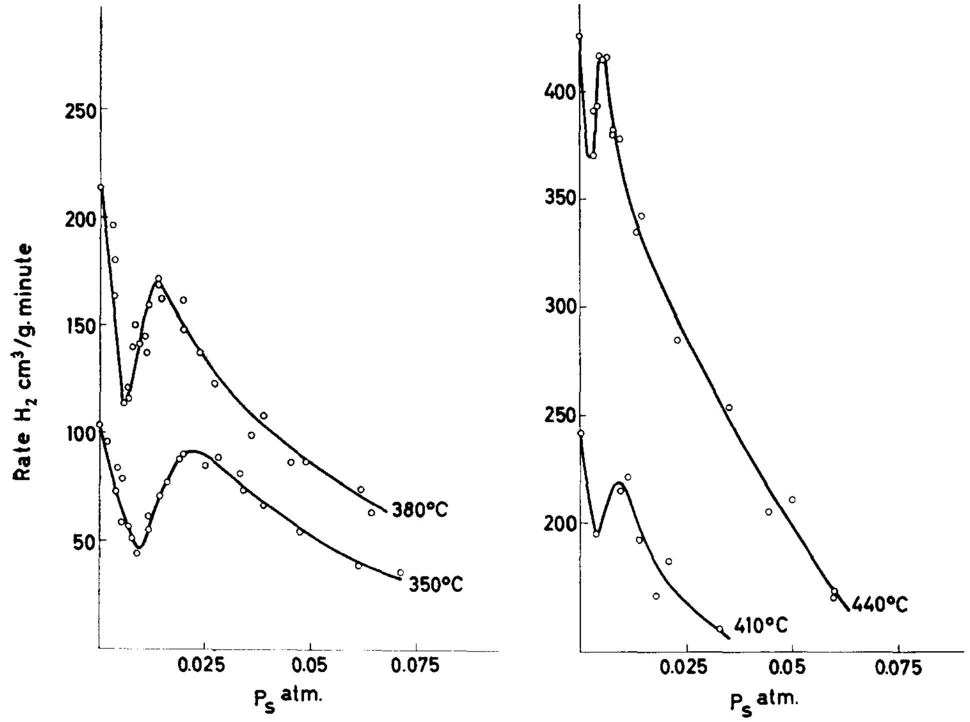

Fig. 6. Reaction rate on $ZnCr_2O_4$ catalyst versus hydrogen partial pressure. Isopropyl alcohol-hydrogen mixture feed.

the equilibrium position.

The voltage applied to the coil is recorded in a Leeds and Northrup recorder.

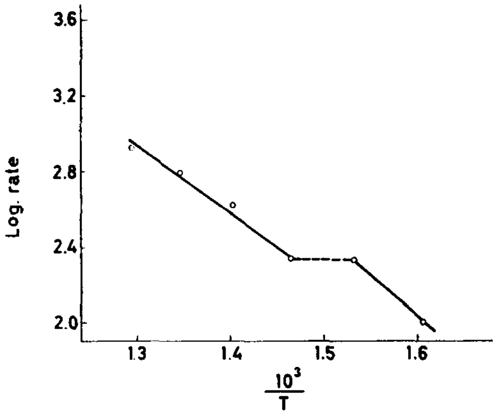

Fig. 7. Dehydrogenation on $ZnCr_2O_4$ catalyst. Arrhenius plot.

The whole system has been calibrated by a buoyancy method and sensitivity is 0.03 mg using a total weight of 10 g.

Experiments can be carried out at different temperatures (kept constant within less than ±1°C) and pressures.

The gas handling system is provided with a McLeod gauge and butyl phthalate and mercury manometers.

Before the experiments were started, the pressure and temperature ranges in which any phenomena may interfere with the measurement, were determined.

Most of the experiments were performed with the same Cr_2O_3 sample, which is capable of being regenerated by the adequate procedure.

Both forms of Cr_2O_3 were prepared by heating the sample in the pan, either in dry air at ~710 mm of Hg or in hydrogen at the same pressure, and 500°C, during several hours and pumping off to a final pressure of less than 10^{-6} mm of Hg. This treatment was repeated until constant pellet weight under vacuum at 500°C was attained.

The adsorption isotherms (see Fig. 8) were obtained starting with the sample, at the desired temperature, under vacuum.

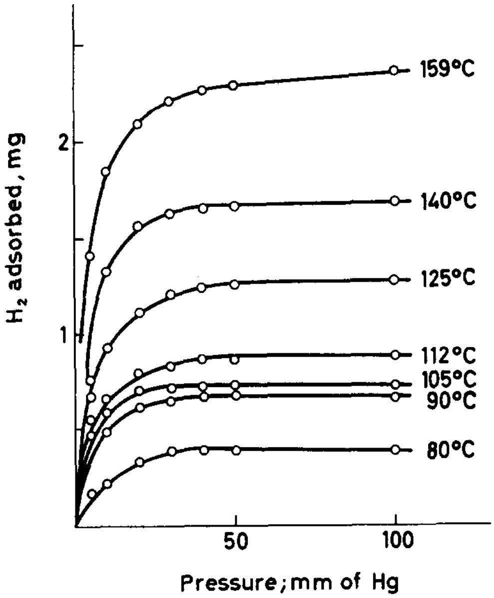

FIG. 8. Adsorption isotherms of H_2 on oxidized Cr_2O_3.

Small amounts of gas were admitted and pressure measured when equilibrium was attained.

In Fig. 9 the logarithm of the maximum weight increase is plotted against $1/T$ for the adsorption of H_2 on oxidized Cr_2O_3.

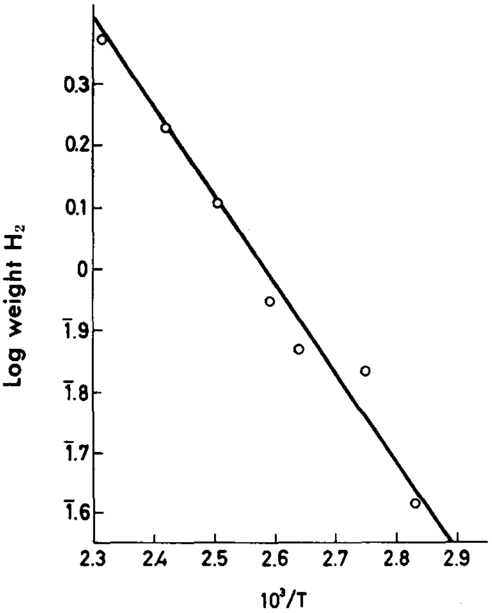

FIG. 9. Logarithmic plot of H_2 weight adsorbed on oxidized Cr_2O_3 versus $1/T$.

The values of ΔH obtained from plots similar to Fig. 9 are given in Table 1.

TABLE 1
ΔH, KCAL/MOLE

Gas	Oxidized Cr_2O_3	Reduced Cr_2O_3
H_2	6.4	4.1
O_2	17.7	4.9

Electrical Resistance of Cr_2O_3

Pajares (*14*) has undertaken the study of the dependence of electrical resistance of Cr_2O_3 on temperature and pressure in different gases, as well as on composition during reaction.

Figure 10 shows a general view of the apparatus employed in the measurement of electrical resistance in gas atmospheres, the main parts of which are as follows:

a. A gas purification and storage system.
b. A circulation pump.
c. An electrical resistance measuring device.
d. The vacuum system and a series of pressure gauges.

The most important parts are the pellet holder and the AC bridge. The Cr_2O_3 pellet is pressed between two platinum electrodes by a glass-covered iron rod, in order to attain pellet-platinum resistances independent of temperature.

The pellet holder is placed in a glass tube, located in an electric furnace. In this way the pellet can be heated up to 550°C. Temperature is electronically controlled within less than ±0.5°C.

The AC bridge has a measuring range from 10^{-2} to 10^{9} Ω and its precision varies according to the measuring region, although it is considered to be higher than ±2%.

Further details on the procedure employed and several tables of experimental values are given in reference (*10*).

The apparatus employed in the study of electrical resistance during the reaction was a combination of that used for measuring catalytic activity (Fig. 1) and the one shown in Fig. 10.

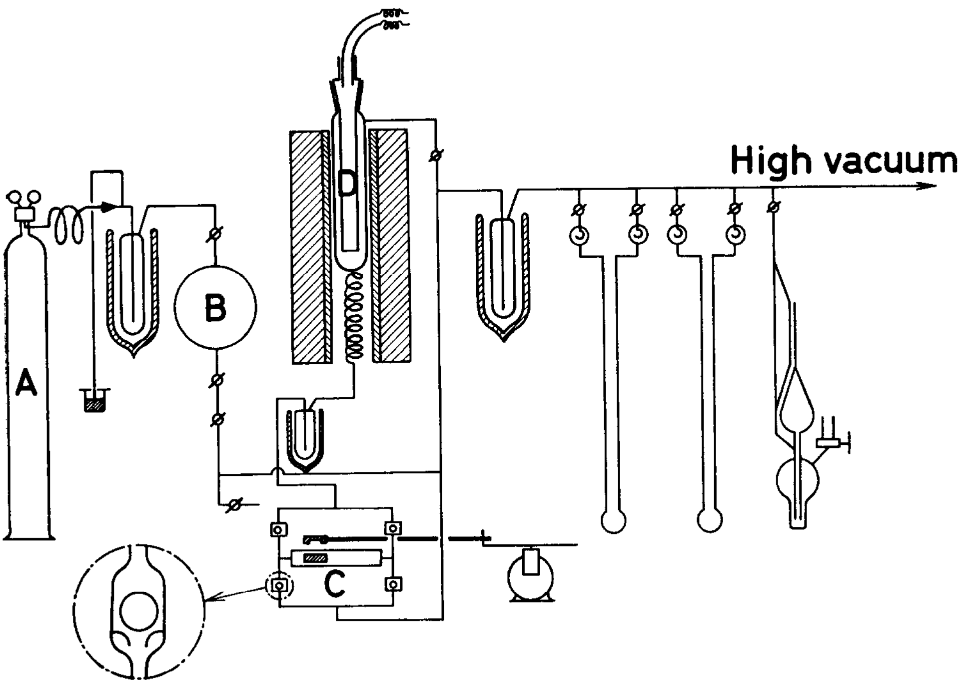

FIG. 10. Schematic diagram of the apparatus for measuring electrical resistance in gases. A—gas tank; B—storage bulb; C—circulation pump; D—pellet holder.

As a general precautionary measure we must indicate that in order to obtain reproducible results the Cr_2O_3 pellets must be either oxidized or reduced at 500°C during long periods of time (several days) and subjected to alternative high vacuum periods.

The study of the change of the conductivity logarithm with $1/T$, using oxidized and reduced Cr_2O_3 pellets and different atmospheres, results in the activation energy values, E, recorded in Table 2.

TABLE 2
E, KCAL/G ATOM OF CARRIERS

Gas	Oxidized Cr_2O_3	Reduced Cr_2O_3
Vacuum ($p < 10^{-6}$ mm of Hg)	11.6	27.9
Air ($p \simeq 700$ mm of Hg)	9.1	—
N_2 ($p \simeq 700$ mm of Hg)	9.1	—
O_2 ($p \simeq 700$ mm of Hg)	9.1	—
H_2 ($p \simeq 700$ mm of Hg)	—	29.7

Figure 11 is a plot of the change in resistance with hydrogen pressure at 500°C. This result agrees very well with the data reported by Voltz and Weller (*15*). The same plot shape has been found at 470 and 440°C.

Figure 12 shows the change in resistance of a Cr_2O_3 pellet at 500°C in a stream of pure isopropyl alcohol. There is a constant resistance region after which resistance decreases with time. After 36 hr resistance attains values of the order of a few thousand ohms. The constant resistance region

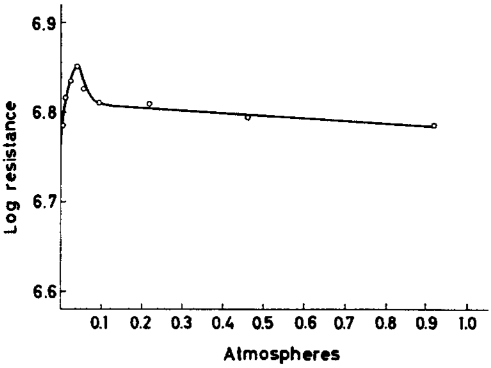

FIG. 11. Change in Cr_2O_3 resistance in function of H_2 pressure. Temperature—500°C.

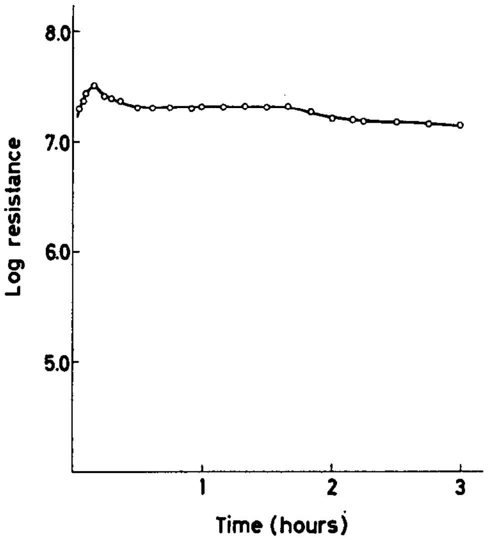

FIG. 12. Change in Cr_2O_3 resistance with time, during the dehydrogenation reaction. Temperature—500°C.

extends through a time lapse which ranges from 30 min to a little less than 2 hr. All resistance measurements taken during the reaction, with the object of studying the influence of hydrogen partial pressure in the feed, have been carried out in this region.

When the resistance attained this constant value, hydrogen was admitted to the stream. Some experimental results are given in Table 3.

The same type of results have been found for 470 and 440°C.

DISCUSSION OF RESULTS

From the shape of the reaction rate versus p_S curves (see Fig. 3) we see that Eq. (*1*) ceases to apply from a certain value of p_S. This behavior is usually characteristic of complex phenomena where at least two simple processes are taking place simultaneously.

We have suggested that these processes are the reactions taking place both on the original *p*-type Cr_2O_3 and on the *n*-type Cr_2O_3, obtained in the reduction of the former (or perhaps by strong ionosorption of hydrogen on the surface). Considering

TABLE 3
RESISTANCE DURING REACTION[a]

Time		Experiment no.					
Hours	Minutes	1	2	3	4	5	6
	10	0.830	—	—	—	—	—
	20	0.742	1.23	1.12	1.13	1.23	0.807
	30	0.742	1.23	1.10	1.12	1.23	0.800
	40	0.733	1.22	1.10[b]	1.16[b]	1.21	0.800
	50	0.742	1.23	1.10	1.19	1.23	0.800
1		0.741	1.23	1.16	1.27	—	—
	10	0.742	1.21	1.20	1.25	—	0.743[b]
	20	0.740	1.22	1.17	1.17	1.13[b]	0.740
	30	0.742	1.23	0.84	1.07	1.13	0.741
	40	0.742	1.23	0.81	0.80	1.13	0.741
	50	0.742	1.21	0.80	0.53	1.13	0.743
2		0.742	1.23	0.77	—	1.13	0.741
	10	0.740	1.21	—	—	1.07	0.741
	20	0.740	1.21	—	—	—	—
	30	0.670	1.21	—	—	—	—
	40	0.650	1.20	—	—	—	—
	50	—	1.15	—	—	—	—
3		0.617	1.00	—	—	—	—

[a] $\Omega \times 10^{-7}$; temperature 500°C.

[b] Before these measurements were performed, hydrogen was admitted in amounts corresponding to the following p_S (atm): experiment no. 3, 0.0045; no. 4, 0.0051; no. 5, 0.0353; no. 6, 0.0774. Experiments nos. 1 and 2 were performed in pure isopropyl alcohol.

the electronic nature of the rate-determining step (be it what it be) the latter ought to display a greater activity due to its *n* character, which is in agreement with the observed increase in the reaction rate.

There is some experimental evidence tending to confirm the existence, in reducing atmospheres, of a Cr_2O_3 modification from the *p* to the *n* type. This type of change has been reported by Voltz and Weller (*15*). Weisz, Prater, and Rittenhouse (*16*) as well as by Chapman and co-workers (*17*). Voltz and Weller measured the resistance of a Cr_2O_3 pellet in hydrogen atmosphere at increasing pressures (temperature 500°C) and found a resistance maximum at about 0.045 atm of hydrogen. The increasing resistance region was associated with *p*-type conductivity, and the fact that the maximum is followed by a decreasing resistance region was attributed to a $p \rightarrow n$ transition. The 0.045 atm value is that for which the maximum occurs, although, of course, transition starts earlier.

Bielanski and co-workers (*18*) have suggested that at temperatures above 450°C and in methanol atmosphere a $p \rightarrow n$ transition is evident in Cr_2O_3.

As excess oxygen imparts nonstoichiometric properties to chromia, reduction would proceed, through an intrinsic stage, to *n*-type cation excess conduction. Obviously this model is an oversimplification since the electronic structure of Cr_2O_3 is more complicated (*19*) than that of a typical extrinsic *p*-type semiconductor.

Available literature is somewhat misleading as regards Cr_2O_3 reduction. A variation in the color from the black oxidized form, to the light green reduced form has been observed when the former is subjected to a temperature of 400°C and a 25 mm of Hg hydrogen pressure. The phenomenon is totally reversible, and under similar conditions the oxidized form is obtained by oxidation of the reduced form.

In proceeding to measure catalytic activities, the originally black pellet acquires a light green color when it has been in the reactor for less than two hours, at a temperature of 440–500°C.

From the reaction rate versus hydrogen partial pressure curves we can assume, in principle, than the $p \rightarrow n$ transition can be experimentally detected only for a given partial pressure. This is not an exception in redox reactions.

If we assume the existence of such a threshold pressure we can understand that the concentration of the surface adsorbed hydrogen, produced during the reaction, would eventually be sufficient for the transition to take place even in the case of a differential reactor and if no hydrogen was introduced in the feed.

This hypothesis may explain the break in the Arrhenius plot found (Fig. 4) in the 410–440°C region; 410°C seems to be a critical temperature for Cr_2O_3 as is shown by the experiments undertaken by Winter (*20*), Bevan, Shelton, and Anderson (*21*), and so on.

We assume that the change experienced by the properties of Cr_2O_3 in this temperature region may be due to a $p \rightarrow n$ transition or to a modification in the structure of *p*-Cr_2O_3 occurring at 410°C and bearing no relation at all to a reduction, as suggested by Winter's work.

However work undertaken by Bhattacharyya and co-workers (*22*) seems to indicate that Cr_2O_3 does not experience any transformation capable of explaining an effect of this type in the temperature range and conditions of our experiments. Nevertheless, if the change experienced by the activation energy were due to a $p \rightarrow n$ transition we could hardly expect minima to appear in the reaction rate versus hydrogen partial pressure curves for the 440°, 470°, and 500°C temperatures. Minima actually occur, although they are much smoother, and occur at lower hydrogen partial pressure, as if part of the reaction had already taken place.

Assuming that both the shape of the reaction rate versus hydrogen partial pressure curves and the inflection in the Arrhenius plots are due to a $p \rightarrow n$ transition, it seems but natural to expect that:

a. Extrapolation of the Arrhenius straight lines for the 440–500°C range to the 350 and 380°C temperatures should

TABLE 4
RATE OF REACTION VALUES ON Cr_2O_3.

Temperature (°C)	p_A (atm)	p_R (atm)	p_S (atm)	V (moles/g min × 10^3)	
				Experimental	Calculated
350	0.92_4	0.000	0.000	$10._3$	9.7_4
	0.86_5	0.000	0.05_9	5.8_1	6.3_0
	0.83_4	0.000	0.09_0	5.0_5	5.1_2
	0.81_5	0.000	0.10_9	4.7_7	4.5_4
380	0.92_7	0.000	0.000	$16._5$	$16._6$
	0.86_2	0.000	0.06_5	9.7_8	$10._1$
	0.84_7	0.000	0.08_0	9.1_6	9.0_8
	0.82_9	0.000	0.09_8	8.3_9	8.0_5
	0.80_6	0.000	0.12_1	7.2_5	6.4_4
	0.78_5	0.000	0.14_2	5.7_6	6.1_0
350	0.83_3	0.09_2	0.000	5.1_4	5.4_3
	0.79_7	0.08_9	0.03_9	3.1_8	3.1_5
	0.78_8	0.08_8	0.04_9	3.0_8	2.8_2
	0.77_9	0.08_7	0.05_9	2.6_6	2.5_3
	0.76_4	0.08_5	0.07_6	1.9_9	2.1_6
380	0.83_3	0.09_3	0.000	8.3_2	8.7_9
	0.79_5	0.08_8	0.04_3	5.8_1	5.5_1
	0.78_2	0.08_7	0.05_7	5.1_2	4.8_1
	0.77_0	0.08_5	0.07_1	4.2_9	4.2_3
	0.76_2	0.08_4	0.08_0	3.6_2	3.9_0
350	0.74_1	0.18_5	0.000	2.1_1	2.6_8
	0.71_4	0.17_9	0.03_3	1.2_6	1.2_4
	0.70_7	0.17_7	0.04_2	1.0_7	0.9_0
	0.69_5	0.17_4	0.05_7	0.7_4	0.6_4
	0.68_1	0.17_0	0.07_5	0.3_5	0.4_1
380	0.73_8	0.18_4	0.000	3.6_3	4.1_8
	0.72_1	0.18_0	0.02_1	3.1_4	3.0_8
	0.71_4	0.17_8	0.03_0	2.9_5	2.7_3
	0.70_7	0.17_6	0.04_2	2.5_7	2.3_4
	0.69_0	0.17_2	0.06_0	2.0_2	1.8_9
	0.67_6	0.17_9	0.07_7	1.4_1	1.5_7
380	0.65_2	0.28_0	0.000	1.9_7	2.3_7
	0.63_9	0.27_4	0.01_9	1.6_3	1.5_8
	0.63_6	0.27_2	0.02_4	1.6_1	1.4_0
	0.62_9	0.27_0	0.03_3	1.3_2	1.2_5
	0.62_2	0.26_7	0.04_3	1.1_1	1.0_6
	0.61_2	0.26_3	0.05_7	0.8_4	0.8_6
	0.60_3	0.25_9	0.07_0	0.6_8	0.7_2

lead to some agreement with the almost linear part of the corresponding reaction versus hydrogen partial pressure plots.

b. Since the same mechanism is accepted for the first part of the reaction rate versus hydrogen partial pressure curve (i.e., before the minimum) at 500°C, an equation of the same type should fit the almost linear region of the reaction rate versus hydrogen partial pressure plot as well as the values extrapolated (for the mixtures with $p_S = 0$) from the Arrhenius plot at high temperatures.

For all the mixtures studied, extrapolated values to 350 and 380°C have been worked out from the high temperature straight lines in the Arrhenius plots.

The parameters of simplified equations, of the same form as Eq. (1) have been fitted by least-squares using these results and experimental points obtained in the p_S region to the right of the reaction rate versus p_S maximum.

In Table 4 both the values calculated from the equations and those obtained experimentally (including the extrapolated ones) are shown.

Agreement is fairly good and seems to substantiate the assumption that there is a $p \rightarrow n$ transition in Cr_2O_3 which is responsible for both the inflection in the Arrhenius plot and the minimum in the reaction rate versus p_S curve.

We must remark that the reaction rate plot shape is found for all the isopropyl alcohol–acetone mixtures for every temperature within this range. The break in the Arrhenius plots has also been found for all feed compositions and, in the case of non-hydrogen-containing mixtures, each experimental point in the plot has been obtained from the rate of reaction versus weight of catalyst linear plots.

In order to confirm these results we thought it would be interesting to study the following:

a. The kinetics on $ZnCr_2O_4$.

b. The adsorption of H_2 and O_2 on Cr_2O_3.

c. The electrical resistance of our Cr_2O_3 pellets in different atmospheres and during the reaction.

Experimental results on $ZnCr_2O_4$ lend further support to the hypothesis of possible $p \rightarrow n$ changes in adequate atmospheres of p-type semiconductors. $ZnCr_2O_4$ is more easily reducible than Cr_2O_3 (see Figs. 6 and 7). Results obtained by Bevan, Shelton, and Anderson (*21*) in oxygen, air, vacuum, and hydrogen atmospheres agree with those obtained by us (*2*, *3*) in the sense that $ZnCr_2O_4$ prepared in air contains oxygen in excess of its stoichiometric value. It is, therefore, a hole semiconductor.

Probably the $p \rightarrow n$ transition in $ZnCr_2O_4$ would be a result of oxygen loss and interstitial Zn^{2+} formation, giving way to a catalyst which, in some respects, would be similar to ZnO.

Adsorption studies (see Table 1) and results on the activation energy of Cr_2O_3 conductivity (see Table 2) both show that the surfaces of the oxidized and reduced form have quite different properties. Furthermore, values in Table 2 may be used in support of the hypothesis which postulates a change in the semiconductor character during reaction.

Results on the variation of resistance with hydrogen pressure, show the same shape as those found by Voltz and Weller (*15*). Figure 11 shows that the p_S value corresponding to the maximum is about 0.05 atm, which is the same for which the reaction rate maximum appears. This strongly favors the hypothesis of a Cr_2O_3 $p \rightarrow n$ change during the reaction.

Finally, results on the variation of the resistance with hydrogen partial pressure in the stream (see Table 3) show that at low hydrogen partial pressure, resistance increases with hydrogen admission. At high partial pressures resistance decreases with increasing p_S. This is further evidence in support of the $p \rightarrow n$ transition.

FINAL REMARKS

It appears that the conception of the transformation of the Cr_2O_3 catalyst in the $p \rightarrow n$ direction, which, as we have seen, has found its way into chemical literature, is not exclusive for Cr_2O_3, but seems to be a property which is common to all semiconductors whenever reaction conditions are adequate. As a matter of fact, we have seen this phenomenon appearing in isopropyl alcohol dehydrogenation on $ZnCr_2O_4$ and Nicolescu and Popescu (*23*) have shown the PtO, Al_2O_3 catalyst (10.8 % PtO) is of a feeble p-type at low temperatures and of the n-type when these are high.

The appearance of a phenomenon of this type introduces a new difficulty in the already complex physical chemistry of catalytic reactions. The phenomenon seems to be interesting from a general standpoint and some of the experimental evidence leads to the conclusion that the overall phenomenon is but incompletely explained. It would therefore be advisable to continue research along these lines in order to attempt its classification.

In this attempt we will face experimental and theoretical difficulties. We would need more accurate measurements of reaction rates at low hydrogen partial pressures and at different total pressures. We would also need accurate surface conductivity and Hall's coefficient measurements avoiding the problems of grain boundaries in a sintered pellet.

From the theoretical standpoint we will face problems connected with carriers mobility in the boundary layer near the surface (*24*), with the possibility that the same molecule be adsorbed either as donor or acceptor (*25*), and so on.

Nevertheless, the better understanding of this problem seems to be important enough to reward us for our effort in overcoming these difficulties.

References

1. Stone, F. S., *in* "Chemistry of the Solid State" (W. E. Garner, ed.), Chapter 15. Butterworths, London 1955.

Hauffe, K., *Advances in Catalysis* **3,** 213 1955.

Gray, T. J., "The Defect Solid State," Chapter 7. Interscience, New York. 1956.

Schwab, G-M., *in* "Semiconductor Surface Physics" (R. H. Kingston, ed.), University of Pennsylvania Press, Philadelphia, p. 283. 1957.

Volkenstein, Th., "Théorie électronique de la Catalyse sur les semi-conductors." Masson, Paris. 1961.

Dowden, D. A., and Wells, D., "Actes du deuxième Congrés International de Catalyse," 1949 (1960).

2. Garner, W. E., Dowden, D. A., and García de la Banda, J. F., *Anales real soc. españ. fís. y quím. Madrid* **50B,** 35 (1954).

3. García, de la Banda, J. F., and Hernáez Marín, J., *Anales real soc. españ. fís. y quím. Madrid* **53B,** 499 (1957).

4. García de la Banda, J. F., and Hernáez Marín, J., *Anales real soc. españ. fís. y quím. Madrid* **54B,** 115 (1958).

5. Hauffe, K., *Angew. Chem.* **67,** 189 (1955).

6. García de la Banda, J. F., and Hernáez Marín, J., *Proceedings of the 3rd International Symposium on the Reactivity of Solids,* **Vol. III,** 59 (1956).

7. García de la Banda, J. F., and Kremenić Orlandini, G., *Anales real soc. españ. fís. y quím. Madrid* **54B,** 85, 97 (1958).

8. Kremenić Orlandini, G., *Anales real soc. españ. fís. y quím. Madrid* **55B,** 465 (1959).

9. García de la Banda, J. F., and Kremenić Orlandini, G., *Anales real soc. españ. fís. y quím. Madrid* **55B,** 477 (1959).

10. García de la Banda, J. F., and Kremenić Orlandini, G., Final Report, Contract No. AF 61(514)-1330, USAF, December, 1960.

11. Germain, J. E., Gras, B., Beaufils, J. P., and Ponsolle, L., *Bull. Soc. Chim. France,* 1172 (1961).

12. Kremenić, G., unpublished results.

13. Azcue, J. M., unpublished results.

14. Pajares, J., unpublished results.

15. Voltz, S. E., and Weller, S. W., *J. Phys. Chem.* **59,** 566, 569 (1955).

Weller, S. W., and Voltz, S. E., *Advances in Catalysis* **9,** 215 (1957).

16. Weisz, P. B., Prater, C. D., and Rittenhouse, K. D., *J. Chem. Phys.* **21,** 2236 (1953).

17. Chapman, R. P., Griffith, R. H., and Marsh, J. D. F., *Proc. Roy. Soc. (London)* **A224,** 419 (1954).

18. Bielanski, A., Derén, J., and Haber, J., *Bull. Acad. Polon. Sci.* **Cl. III, Vol. III**(9), 479 (1955); ibid., **Cl. III, Vol. IV**(8), 533 (1956); *Nature* **179,** 668 (1957).

Derén, J., Haber, J., and Mrowec, S., *Bull. Acad. Polon. Sci.* **Cl. III, Vol. IV**(4), 107 (1956).

19. Hauffe, K., and Block, J., *Z. physik. Chem.* **198,** 232 (1951).

20. Winter, E. R. S., *Discussions Faraday Soc.* **No. 8,** 231 (1950).

21. Bevan, D. J. M., Shelton, J. P., and Anderson, J. S., *J. Chem. Soc.* 1729 (1948).

22. Bhattacharyya, S. K., and Ramachandran, V. S., *in* "Advances in Catalysis," **9,** 114 (1957).

Bhattacharyya, S. K., and Kameswari, S., *J. Chim. Phys.* **56,** 823 (1959).

23. Nicolescu, I. V., and Popescu, Al., *Acad. rep. populare Romine Studii certerari chim.* **7,** 49 (1959).

24. Schrieffer, J. R., *in* "Semiconductor surface physics" (R. H. Kingston, ed.), p. 55. University of Pennsylvania Press, Philadelphia, 1957.

25. Wolkenstein, Th., *J. Chim. Phys.* **54,** 175 (1957).